Conclusions. Our study is part of recent attempts in "neuroeconomics" and the "cognitive neuroscience of social behavior" to understand the social brain and the associated moral emotions (37–44). However, this study sought to identify the neural basis of the altruistic punishment of defectors. The ability to develop social norms that apply to large groups of genetically unrelated individuals and to enforce these norms through altruistic sanctions is one of the distinguishing characteristics of the human species. Altruistic punishment is probably a key element in explaining the unprecedented level of cooperation in human societies (1–3). We hypothesize that altruistic punishment provides relief or satisfaction to the punisher and activates, therefore, reward-related brain regions. Our design generates five contrasts in which this hypothesis can be tested, and the anterior dorsal striatum is activated in all five contrasts, which suggests that the caudate plays a decisive role in altruistic punishment. Caudate activation is particularly interesting because this brain region has been implicated in making decisions or taking actions that are motivated by anticipated rewards (17–20). The prominent role of the caudate in altruistic punishment is further supported by the fact that those subjects who exhibit stronger caudate activation spend more money on punishing defectors. Moreover, our results also shed light on the reasons behind this correlation. Subjects who exhibit higher caudate activation at the maximal level of punishment if punishment is costless for them also spend more resources on punishment if punishment becomes costly. Thus, high caudate activation seems to be responsible for a high willingness to punish, which suggests that caudate activation reflects the anticipated satisfaction from punishing defectors. Our results therefore support recently developed social preference models (6–8), which assume that people have a preference for punishing norm violations, and illuminate the proximate mechanism behind evolutionary models of altruistic punishment.

References and Notes
1. R. Boyd, H. Gintis, S. Bowles, P. J. Richerson, *Proc. Natl. Acad. Sci. U.S.A.* **100**, 3531 (2003).
2. S. Bowles, H. Gintis, *Theor. Popul. Biol.* **65**, 17 (2004).
3. E. Fehr, S. Gächter, *Nature* **415**, 137 (2002).
4. E. Sober, D. S. Wilson, *Unto Others: The Evolution and Psychology of Unselfish Behavior* (Harvard University Press, Cambridge, MA, 1998).
5. E. Fehr, U. Fischbacher, *Nature* **425**, 785 (2003).
6. M. Rabin, *Am. Econ. Rev.* **83**, 1281 (1993).
7. E. Fehr, K. M. Schmidt, *Q. J. Econ.* **114**, 817 (1999).
8. C. F. Camerer, *Behavioral Game Theory: Experiments in Strategic Interaction* (Princeton University Press, Princeton, NJ, 2003).
9. W. Schultz, *Nature Rev. Neurosci.* **1**, 199 (2000).
10. P. Apicella, T. Ljungberg, E. Scarnati, W. Schultz, *Exp. Brain Res.* **85**, 491 (1991).
11. O. Hikosaka, M. Sakamoto, S. Usui, *J. Neurophysiol.* **61**, 814 (1989).
12. M. R. Delgado, V. A. Stenger, J. A. Fiez, *Cereb. Cortex* **14**, 1022 (2004).
13. B. Knutson, A. Westdorp, E. Kaiser, D. Hommer, *Neuroimage* **12**, 20 (2000).
14. C. Martin-Soelch, J. Missimer, K. L. Leenders, W. Schultz, *Eur. J. Neurosci.* **18**, 680 (2003).
15. M. R. Delgado, H. M. Locke, V. A. Stenger, J. A. Fiez, *Cognit. Affect. Behav. Neurosci.* **3**, 27 (2003).
16. B. Knutson, C. M. Adams, G. W. Fong, D. Hommer, *J. Neurosci.* **21**, RC159 (2001).
17. W. Schultz, R. Romo, *Exp. Brain Res.* **71**, 431 (1988).
18. R. Kawagoe, Y. Takikawa, O. Hikosaka, *Nature Neurosci.* **1**, 411 (1998).
19. J. R. Hollerman, L. Tremblay, W. Schultz, *J. Neurophysiol.* **80**, 947 (1998).
20. J. O'Doherty *et al.*, *Science* **304**, 452 (2004).
21. Materials and methods are available as supporting material on *Science* Online.
22. To maintain symmetry with case 1, player B can also give half of his money to A if A does not trust him. However, because all subjects (except one) in the role of A trusted B, this contingency almost never occurred.
23. In all conditions, both players received an additional endowment of 20 MUs after player B made his decision. This endowment allowed A to finance the cost of punishment in those conditions in which punishment was also costly for him. If A did not punish, both players kept the 20 MUs. If punishment was not costly for A, he kept the 20 MUs regardless of the number of assigned punishment points.
24. J. A. Salinas, N. M. White, *Behav. Neurosci.* **112**, 812 (1998).
25. M. J. Koepp *et al.*, *Nature* **393**, 266 (1998).
26. M. R. Delgado, L. E. Nystrom, C. Fissell, D. C. Noll, J. A. Fiez, *J. Neurophysiol.* **84**, 3072 (2000).
27. H. C. Breiter *et al.*, *Neuron* **19**, 591 (1997).
28. E. A. Stein *et al.*, *Am. J. Psychiatr.* **155**, 1009 (1998).
29. E. K. Miller, J. D. Cohen, *Annu. Rev. Neurosci.* **24**, 167 (2001).
30. A. D. Wagner, A. Maril, R. A. Bjork, D. L. Schacter, *Neuroimage* **14**, 1337 (2001).
31. D. C. Krawczyk, *Neurosci. Biobehav. Rev.* **26**, 631 (2002).
32. A. Bechara, H. Damasio, A. R. Damasio, *Cereb. Cortex* **10**, 295 (2000).
33. N. Ramnani, A. M. Owen, *Nature Rev. Neurosci.* **5**, 184 (2004).
34. R. Elliott, J. L. Newman, O. A. Longe, J. F. Deakin, *J. Neurosci.* **23**, 303 (2003).
35. F. S. Arana *et al.*, *J. Neurosci.* **23**, 9632 (2003).
36. C. D. Batson, J. Fultz, A. Schoenrade, A. Paduano, *J. Pers. Soc. Psychol.* **53**, 594 (1987).
37. R. Adolphs, *Curr. Opin. Neurobiol.* **11**, 231 (2001).
38. J. D. Greene, R. B. Sommerville, L. E. Nystrom, J. M. Darley, J. D. Cohen, *Science* **293**, 2105 (2001).
39. K. McCabe, D. Houser, L. Ryan, V. Smith, T. Trouard, *Proc. Natl. Acad. Sci. U.S.A.* **98**, 11832 (2001).
40. J. K. Rilling *et al.*, *Neuron* **35**, 395 (2002).
41. T. Singer *et al.*, *Neuron* **41**, 653 (2004).
42. J. Moll *et al.*, *J. Neurosci.* **22**, 2730 (2002).
43. A. G. Sanfey, J. K. Rilling, J. A. Aronson, L. E. Nystrom, J. D. Cohen, *Science* **300**, 1755 (2003).
44. R. Adolphs, *Nature Rev. Neurosci.* **4**, 165 (2003).
45. We gratefully acknowledge support by the University of Zurich, the Swiss National Science Foundation, and the MacArthur Foundation Network on Economic Environments and the Evolution of Individual Preferences and Social Norms. We thank R. Adolphs, T. Singer, and L. Jäncke for helpful comments on earlier drafts of this paper.

Spatial Representation in the Entorhinal Cortex

Marianne Fyhn,[1] Sturla Molden,[1] Menno P. Witter,[1,2] Edvard I. Moser,[1]* May-Britt Moser[1]

As the interface between hippocampus and neocortex, the entorhinal cortex is likely to play a pivotal role in memory. To determine how information is represented in this area, we measured spatial modulation of neural activity in layers of medial entorhinal cortex projecting to the hippocampus. Close to the postrhinal-entorhinal border, entorhinal neurons had stable and discrete multipeaked place fields, predicting the rat's location as accurately as place cells in the hippocampus. Precise positional modulation was not observed more ventromedially in the entorhinal cortex or upstream in the postrhinal cortex, suggesting that sensory input is transformed into durable allocentric spatial representations internally in the dorsocaudal medial entorhinal cortex.

An extensive body of evidence suggests that the hippocampus is essential for fast encoding and storage of new episodic memories but has a more limited role in remote memory, which is thought to be stored primarily in the neocortex (1–4). Memory consolidation in the neocortex appears to be a slow and gradual process based on repeated interactions with the hippocampus (2, 3). These interactions must be mediated largely through the entorhinal cortex, which interconnects the hippocampus with nearly all other association cortices (5–8). Understanding how information is processed in the entorhinal cortex is thus essential to resolving the interaction between the hippocampus and neocortex during encoding, consolidation, storage, and retrieval of memory.

However, little is known about how sensory input is represented in the entorhinal cortex. Although hippocampal memories are expressed at the neuronal level as representations with evident correlates to the spatial and nonspatial structure of the external environment (6, 9, 10), the functional correlates of entorhinal neurons

[1]Centre for the Biology of Memory, Medical-Technical Research Centre, Norwegian University of Science and Technology, 7489 Trondheim, Norway. [2]Research Institute Neurosciences, Department of Anatomy, VU University Medical Center, Amsterdam, Netherlands.

*To whom correspondence should be addressed. E-mail: edvard.moser@cbm.ntnu.no

are less manifest. Recordings from parahippocampal areas that provide input to the hippocampus suggest that neurons in these regions are only weakly modulated by the position of the animal (11–15). The contrast between the weak spatial input signal and the strong spatial output signal from the hippocampus has been taken as evidence for intrahippocampal computation of allocentric location (11, 12) and a fundamental involvement of the hippocampus in spatial navigation (9).

The attribution of spatial algorithms to the hippocampus rests on the assumption that the upstream parahippocampal cortices have been adequately sampled. The parahippocampal cortex comprises a number of subregions with topographically organized internal and external connections, suggesting a modular organization (7, 8, 16, 17). The entorhinal cortex, for example, segregates into overlapping recurrently connected bands parallel to the rhinal sulcus that cut across the medial and lateral subdivisions of the area (7, 16, 17) (Fig. 1A). The most dorsolateral band provides the strongest input to the dorsal part of the hippocampus (7, 16), which has the sharpest and most information-rich place fields (18) and plays a more essential role in spatial learning than the ventral hippocampus (19, 20). This dorsolateral band also receives most of the visuospatial input to the entorhinal cortex (8). Yet none of the previous recordings suggesting weak spatial modulation in entorhinal cortex were made in this dorsolateral band (11–13). Thus, we reexamined spatial representation upstream of the hippocampus by recording along the entire dorsolateral-to-ventromedial axis of the medial entorhinal cortex (MEC) (21).

Topographical organization of entorhinal-hippocampal connections. We first labeled the projections to the hippocampus that arise in the dorsolateral band portion of MEC with the use of the anterogradely transported tracer biotinylated dextrane amine (BDA) (Fig. 1B). Likewise, we visualized the projections originating from the ventromedial band portion of MEC in the same sagittal plane (Fig. 1C). All dorsolateral injections (n = 3) resulted in strong anterograde labeling exclusively in the dorsal hippocampus, with labeling limited to well-defined portions of the molecular layer of the dentate gyrus and subiculum, and stratum lacunosum-moleculare of CA3 and CA1 (Fig. 1B; supporting online text). Injections in the ventromedial band portion of MEC (n = 3) produced labeling exclusively in the ventral hippocampus but with a comparable distribution in layers and fields (Fig. 1C). These observations indicate topographically organized projections from MEC to the hippocampus with a dorsolateral-to-ventromedial axis of origin in MEC corresponding to the dorsal-to-ventral axis of the hippocampus (16, 22).

Heterogeneity of spatial firing in entorhinal cortex. A total of 220 putative

excitatory cells in layers II and III were recorded from 14 rats with electrodes in the dorsolateral (n = 10; Figs. 1A and 2A), intermediate (n = 1; Figs. 1A and 3A), or ventromedial (n = 3; Figs. 1A and 3C) bands of MEC, with the dorsolateral and ventromedial recording locations matching the tracer injection sites. Spike activity was recorded while rats collected food in a square enclosure (21). In the dorsolateral band, putative excitatory cells had sharp and coherent place fields in the test box (Figs. 2B and 4; n = 135). Nearly all cells had multiple firing fields (with a median number of 4; Fig. 4E), but individual fields were clearly delimited against the intervening background. Firing was only weakly modulated by the rat's direction of movement

(Figs. 2C and 4K). The multiple firing fields of a cell showed a remarkably dispersed distribution compared to a shuffled distribution (Fig. 2D). The distance between neighboring fields was larger than expected from a uniform random distribution (Wilcoxon signed-ranks test: $Z = 9.0$, $P < 0.001$), and the range was narrower ($Z = 5.6$, $P < 0.001$). The location of the fields was generally consistent across trials and days (Figs. 2B and 4J; fig. S1). The number of subfields was unrelated to the confidence with which the unit could be separated from other units recorded on the same tetrode (figs. S2 and S3).

We compared place fields of these dorsolateral cells with those of cells in intermediate (n =

Fig. 1. Topographic projections from MEC to hippocampus. (**A**) Ventral-posterior view of a whole rat brain showing the outline of the left entorhinal cortex (colored surface) and the rhinal fissure (stippled gray line). The dorsolateral-to-ventromedial gradient of entorhinal extrinsic connectivity (magenta-to-blue) cuts across both lateral and medial entorhinal subdivisions (border indicated by yellow line). Filled white markers indicate sites of tracer injection in (B) and (C). Open white markers indicate injections not illustrated. Filled yellow markers show recording positions in Figs. 2A, 3A, 3C, and 5E. Open yellow markers indicate selected additional recording positions in MEC. (**B**) Sagittal sections illustrating the projections from the dorsolateral-band zone of MEC to the hippocampus. (Left) Injection site of BDA. Dorsal and ventral borders of MEC are indicated by red lines. (Middle) Low-power brightfield sagittal section showing dense staining in dorsal but not ventral hippocampus (black arrowheads indicate borders between hippocampal subfields). (Right) High-power darkfield photomicrographs of indicated areas in the dorsal and ventral hippocampus. (Top right) Bright orange band corresponds to dense labeling in the middle molecular layer of the dentate gyrus (red arrow) (21). The labeling more dorsally (yellow arrow) corresponds to the less massive termination of MEC fibers in the proximal half of CA1. (**C**) Projections from the ventromedial region of MEC. Note the absence of staining in dorsal hippocampus (darkfield picture, top right) and moderate labeling in fields CA1 and dentate gyrus of the ventral hippocampus (darkfield picture, bottom right; yellow and red arrows, respectively) (21).
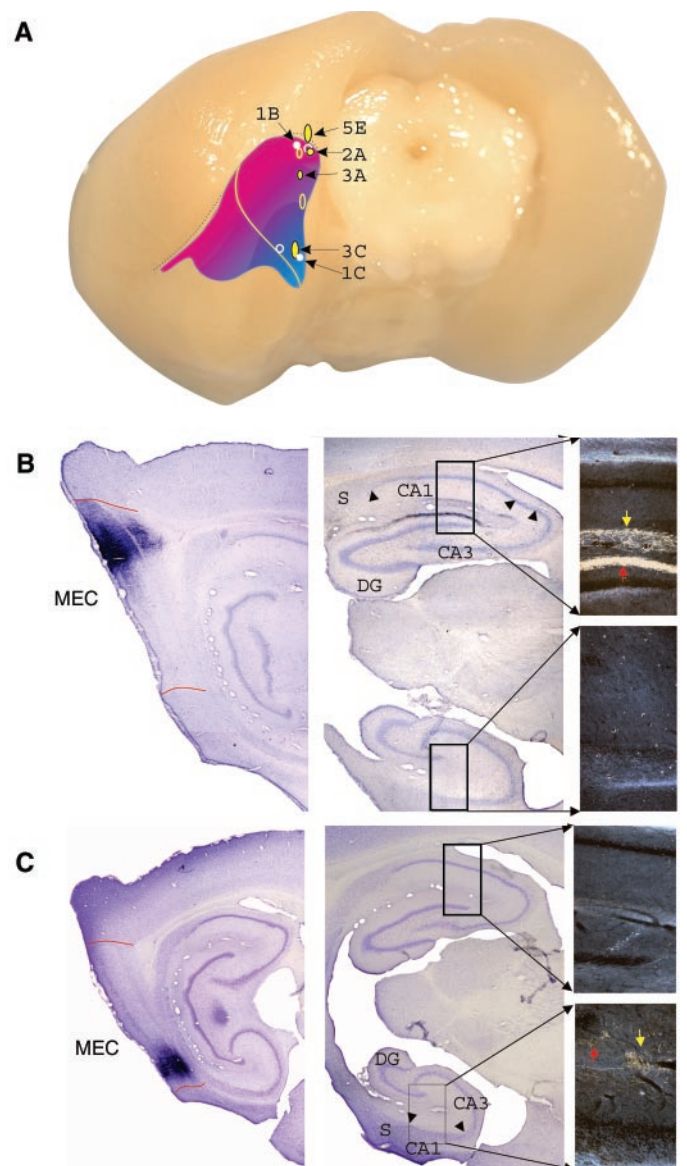
22) and ventromedial ($n = 63$) parts of MEC. At intermediate positions, most cells were spatially modulated, but their fields were broader and less coherent and lacked the characteristic intervening silent areas of the multipeaked fields in the dorsolateral band (median number of fields: 1.75; Figs. 3B and 4). At the most ventromedial positions, only very weak spatial modulation was apparent (Figs. 3D and 4), even in cells classified as clearly separated from their peers (fig. S2C).

Quantitative analyses confirmed that the neuronal response to location differed along the dorsolateral-to-ventromedial axis of MEC. The spatial information rate in bits/s of all cells recorded in MEC correlated significantly with the position of the recording electrode along the dorsolateral-to-ventromedial axis ($r = 0.78$; $n = 14$ rats; $P = 0.001$). Information rates in the dorsolateral, intermediate, and ventromedial bands were strikingly different, with a significantly larger proportion of high–information rate cells in the dorsolateral band [Fig. 4I; Kruskal-Wallis test: $\chi^2(2) = 111.1$, $P < 0.001$; supporting online text]. Cells in the dorsolateral band had a larger number of nonoverlapping firing fields per cell [Fig. 4E; $\chi^2(2) = 103.8$; $P < 0.001$]. These fields were smaller [Fig. 4F; $\chi^2(2) = 31.9$, $P < 0.001$] and more coherent [Fig. 4H; $\chi^2(2) = 117.5$, $P < 0.001$] than in the intermediate and ventromedial band, and the

peak rates were higher [Fig. 4D; $\chi^2(2) = 81.2$; $P < 0.001$]. The collective activity of a small number of simultaneously recorded dorsolateral cells was sufficient to reconstruct accurately the trajectory of the rat (23) (movie S1). The fields were correlated across trials at all dorsolateral-to-ventromedial levels, but the stability was higher in the dorsolateral band [Fig. 4J; $\chi^2(2) = 27.7$, $P < 0.001$]. Modulation by the rat's direction of movement was weak in all regions (Fig. 4K; $\chi^2 = 0.3$; not significant).

Comparison with target areas in the hippocampus. The positional firing properties of the superficial dorsolateral band neurons suggest that spatial location is expressed accurately before signals enter the hippocampus. We compared directly the firing fields of cells in the dorsolateral band of MEC (10 rats) with those of simultaneously recorded cells in the connectionally related portion of dorsal CA 1 (3 rats; 56 cells) (Figs. 1B and 4). Sharply defined place fields predominated in both cell groups. The average information rate in bits/s was not different (Wilcoxon rank-sum test: $Z = 1.47$; $n = 114$), nor was the spatial coherence of the firing ($Z = 1.44$). However, the number of subfields per cell was larger in MEC than in CA1 ($Z = 2.75$, $P < 0.01$), the subfields were slightly smaller ($Z = 1.96$, $P = 0.05$), and the peak rate was higher ($Z = 2.80$, $P < 0.005$). Modulation by direction of movement was lower in MEC

than in CA1 ($Z = 4.23$, $P < 0.001$). Firing rate maps were stable between trials in both areas, but were less in MEC than in CA1 ($Z = 3.73$, $P < 0.001$; Fig. 4 and fig. S1B).

Spatial firing fields after removal of hippocampal output. Output from the hippocampus to deep layers of MEC may influence neuronal firing in superficial layers (7, 17, 24). The precise spatial firing of layer II and III neurons in the dorsocaudal MEC may therefore be influenced by operations taking place within the hippocampus. We examined the spatial firing of 30 MEC neurons in five postoperatively trained rats with selective bilateral hippocampal lesions. In four rats, the lesions were complete throughout the dorsal 80 to 100% of the hippocampus (Fig. 5A). The fifth rat had a complete lesion of CA3 and CA1 (Fig. 5C). All five rats had cells with discrete multipeaked place fields in layer II of the dorsolateral band (Fig. 5, B and D). The lesions had no significant effect on the spatial information rate (lesioned rats: 0.62; control rats: 0.72; $Z = 1.53$), the median number of peaks (3.5 versus 4; $Z = 1.07$), or the mean field size (0.19 m² versus 0.13 m²; $Z = 1.38$) (compare with Fig. 4, A and B). However, they decreased the spatial coherence (0.47 versus 0.70; $Z = 5.2$, $P < 0.001$) and the dispersedness of the firing
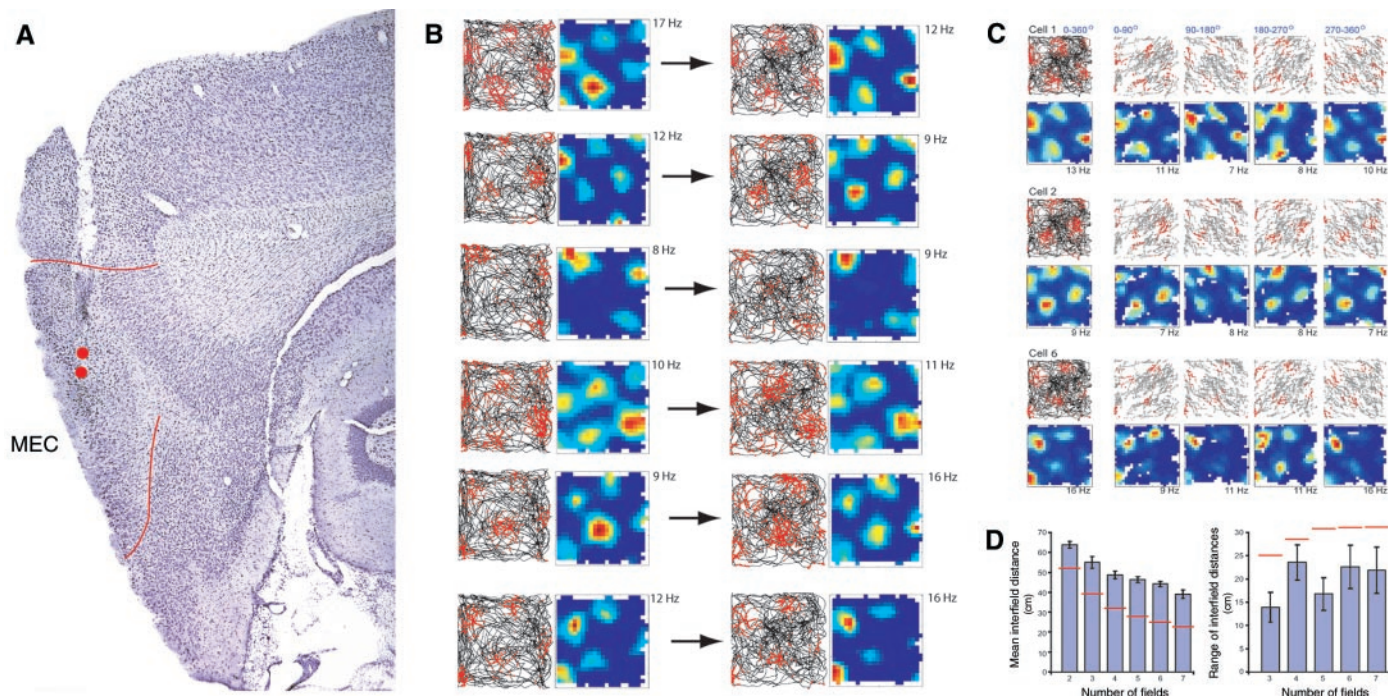

Fig. 2. Discrete multipeaked firing fields in putative excitatory cells in the dorsolateral band of MEC. (**A**) Nissl stain showing electrode locations in layers III (upper red circle) and II (lower red circle) of the dorsolateral band (sagittal section; see also Fig. 1A). Red lines indicate borders of MEC toward postrhinal cortex (dorsal) and parasubiculum (ventral). (**B**) Firing fields of simultaneously recorded cells from the lower location in (A). Each row shows one cell, and each pair of columns one trial. The trajectory with superimposed spikes (red) is shown to the left in each pair of columns; the corresponding color-coded rate map (with the peak rate) appears to the right. The color scale is linear with blue as zero and red as maximum. Regions not covered by the rat are in white. Note the multiple discrete firing fields that were stable across trials. (**C**) Trajectory maps and color-coded maps showing similar fields for each directional quadrant of body movement for three of the cells in (B). (**D**) Distance between neighboring firing fields in dorsolateral-band cells with more than two fields (all rats; mean, SEM, and range for each cell). Red lines indicate chance level.

fields (distance between neighboring fields: 39.8 cm versus 49.5 cm; $Z = 3.7$, $P < 0.001$), although the fields were still more dispersed than expected from a uniform random distribution (39.8 cm versus 32.2 cm; $Z = 4.1$, $P < 0.001$). The firing also became more dependent on the direction of movement (directionality index: 0.49 versus 0.21; $Z = 5.3$, $P < 0.001$), and the spatial correlation between trials declined (0.37 versus 0.70; $Z = 1.86$, $P < 0.05$, one-tailed Wilcoxon test).

Absence of discrete firing fields further upstream. To determine whether precise spatial information arises in MEC or is relayed from other areas, we recorded activity from the connectionally related parts of layers III and V of the postrhinal cortex, which represent the major source of visuospatial input to the dorsolateral band of MEC (8). Spikes were recorded from 48 well-isolated cells with broad waveforms in three rats (Fig. 5, E to G). The firing fields generally covered the entire recording environment (median field size: 0.55 m²). Information rates were low (median 0.18 bits/s), as was the average stability of the spatial firing across trials (median correlation 0.25). No difference was observed between layers III and V. In one rat, the electrodes were turned into the dorsolateral band of MEC subsequent to postrhinal cortex (Fig. 5E). Sharp, multipeaked firing fields appeared as soon as the electrodes moved into entorhinal cortex (Fig. 5H).

Discussion. Our data provide functional evidence for a modular organization of MEC (7, 8, 16, 17). Allocentric view–independent spatial information is expressed primarily by neurons close to the border with the postrhinal cortex. This part of MEC is the predominant recipient of visuospatial information from the visual and parietal cortices (8). At more intermediate regions, firing fields get more dispersed, as reported previously (11–13). The near absence of position-modulated neurons in the most ventromedial region is consistent with the preponderantly nonspatial input to this area (7, 8). The differences in spatial firing within MEC provide a rationale for the dominant involvement of the dorsal part of the hippocampus in spatial memory (19, 20).

The fact that information about the rat's current location was expressed as strongly in superficial layers of the dorsocaudal MEC as in the hippocampus suggests that major steps in the computation of allocentric space occur upstream of the hippocampus (25). Although a single multipeaked entorhinal place field provides little information about the animal's location, the sharp and consistent delineation of individual peaks from the background permits the current position of the animal to be represented accurately by the collective firing of only a small number of superficial MEC neurons (23, 26). Hippocampal return projections were not required to maintain the information-rich multipeaked firing pattern, but reverberation through the hippocampus appeared to strengthen the separation and directional independence of the firing fields (27).

Spatial information in the dorsocaudal MEC may be derived from afferent cell populations such as the postrhinal cortex and the dorsal presubiculum, which project heavily to superficial layers of the dorsolateral band of MEC (8, 28). However, spatial modulation in the postrhinal cortex was weak and unstable (15). A similar insensitivity to allocentric location has been noted in the dorsal presubiculum, in which neurons are strongly modulated by head direction (29), and in areas with less extensive projections to the dorsolateral band of MEC (14, 30). These observations suggest that spatial signals are actively transformed into cohesive allocentric representations within the entorhinal cortex itself. This transformation may also calibrate positional information with head-direction input from the dorsal presubiculum. Inputs from the dorsal presubiculum target a substantial proportion of excitatory neurons in the superficial layers of the dorsolateral band of MEC (28). Lesions of the dorsal presubiculum impair the directional control of polarizing stimuli on hippocampal place cells (31), implying that the dorsal hippocampus receives a conjunction of positional and directional input from MEC.
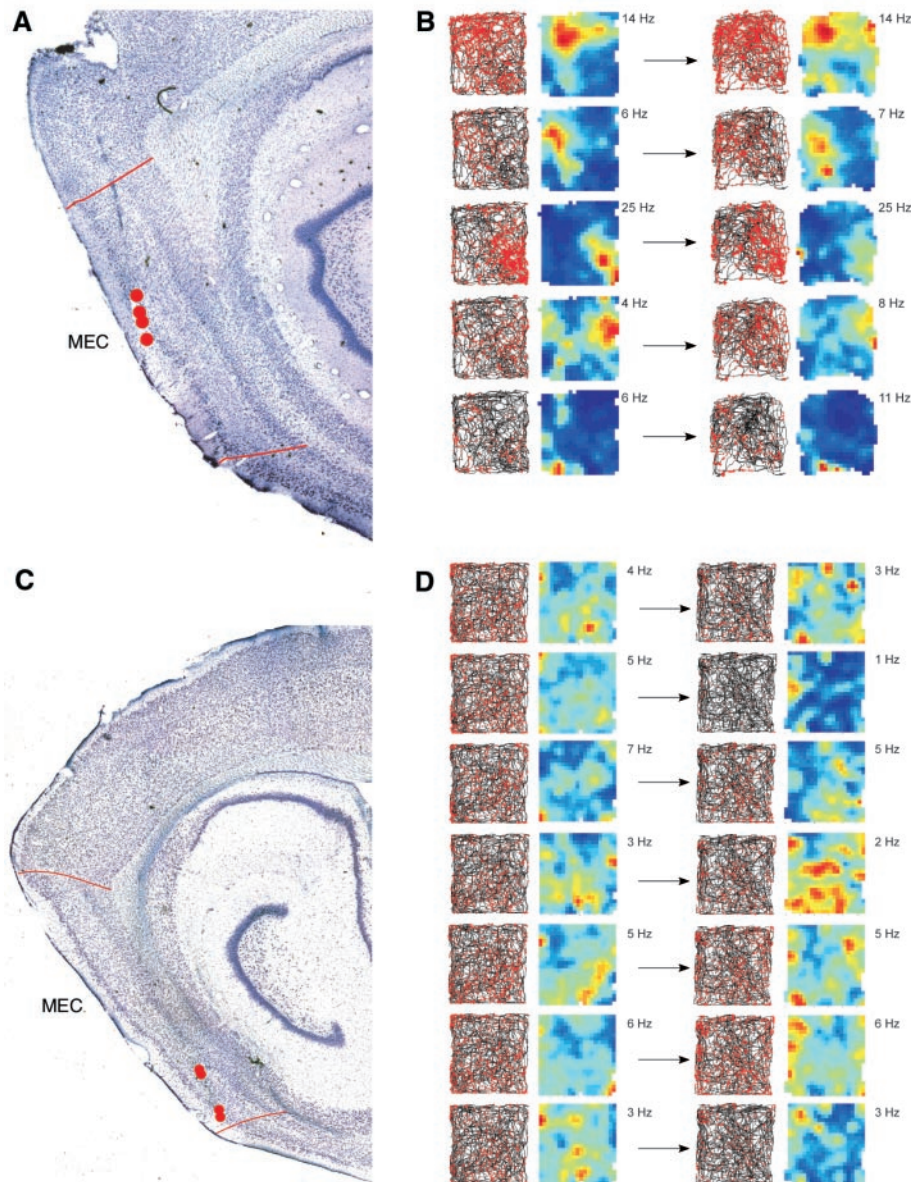

Fig. 3. Weak spatial modulation in the intermediate band (**A**) and absence of spatial modulation in the ventromedial band (**C**) of MEC. Sagittal sections indicating recording locations of layer II in the intermediate band [red circles in (A)] and in layers III and II of the ventromedial band [upper and lower red circles in (C), respectively] (see also Fig. 1A). Borders of MEC are indicated by red lines. (**B** and **D**) Firing fields of simultaneously recorded cells in layer II of the intermediate or ventromedial band [(B) and (D), respectively].
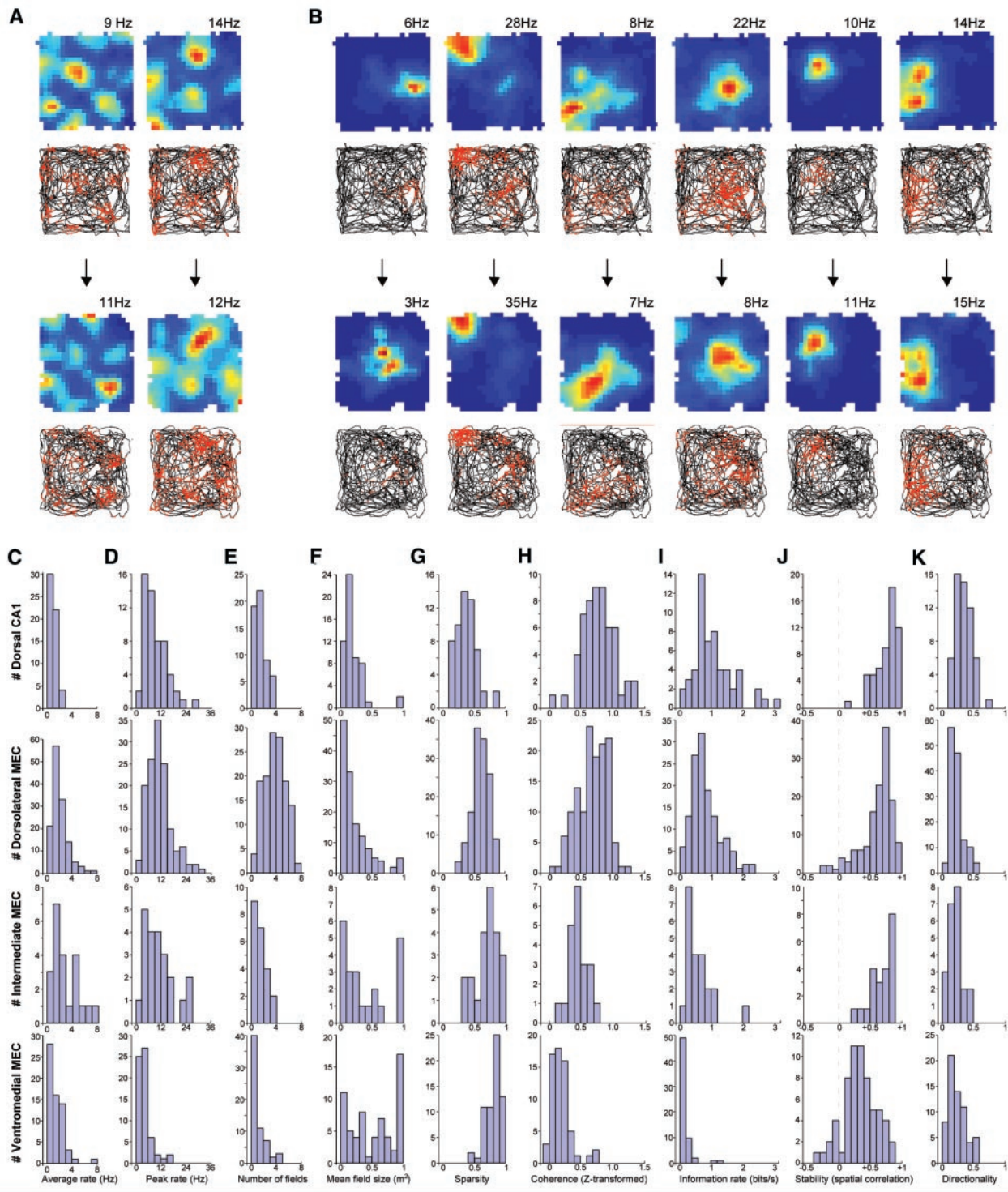
Fig. 4. Spatial modulation in superficial layers of MEC compared to hippocampal area CA1. (**A** and **B**) Color-coded rate maps and trajectory maps for cells recorded simultaneously from layer II in the dorsolateral band (A) and dorsal CA1 of the contralateral hippocampus (B). Each column shows one cell. The top two rows show trial 1; the bottom two rows show trial 2. (**C** to **K**) Quantitative analysis of spatial modulation in putative excitatory cells of layers II and III in dorsolateral, intermediate, and ventromedial bands of MEC as compared to pyramidal cells in dorsal CA1 (all cells in all regions). Panels show distribution of average rate (C), peak rate (D), number of fields (E), mean field size (F), sparsity (G), spatial coherence (H), spatial information rate (I), stability (J), and modulation by movement direction (K) (*21, 23*).

Although our data show that the animal's current location is represented accurately upstream of the hippocampus, there were several noticeable differences between the spatial codes in MEC and hippocampus. First, place fields were slightly more stable across trials in the hippocampus. Although some cells fired repeatedly at exactly the same locations in both areas, new or dislocated fields were more common in MEC, pointing to a stronger involvement of the hippocampus in storage or retrieval of the afferent information. Unlike the MEC, the hippocampus may store information in such a manner that the same representation can be retrieved even with slight fluctuation of the retrieval cues across

Fig. 5. Spatial firing in the dorsolateral band may reflect intrinsic computations of the MEC. (**A** to **D**) Spatial modulation in the dorsolateral band of MEC in two rats with ibotenate lesions of the hippocampus (three sagittal levels from lateral to medial). The rat in (A) and (B) had a complete lesion of CA3, CA1, dentate gyrus, and subiculum; the one in (C) and (D) had a complete lesion of CA3 and CA1, but dentate gyrus and subiculum were partly spared. Red circles indicate electrode locations in layer II; red lines indicate borders of MEC. Both animals had cells with discrete multi-peaked firing fields, but the coherence of the fields was reduced. (**E** to **H**) Absence of strong spatial modulation upstream in adjacent postrhinal cortex. (E) Sagittal section through the postrhinal cortex (POR) and MEC indicating recording locations (red circles) and regional borders (parasubiculum, PaS; presubiculum, PrS; see also Fig. 1A). Note that two recording locations were in POR (layers V and III) and one in MEC (layer III). (F and G) Dispersed and unstable firing fields of postrhinal broadwaveform cells at the upper (F) and lower (G) recording position in POR. (H) Multiple discrete firing fields in a layer-III neuron at the succeeding recording position in MEC.
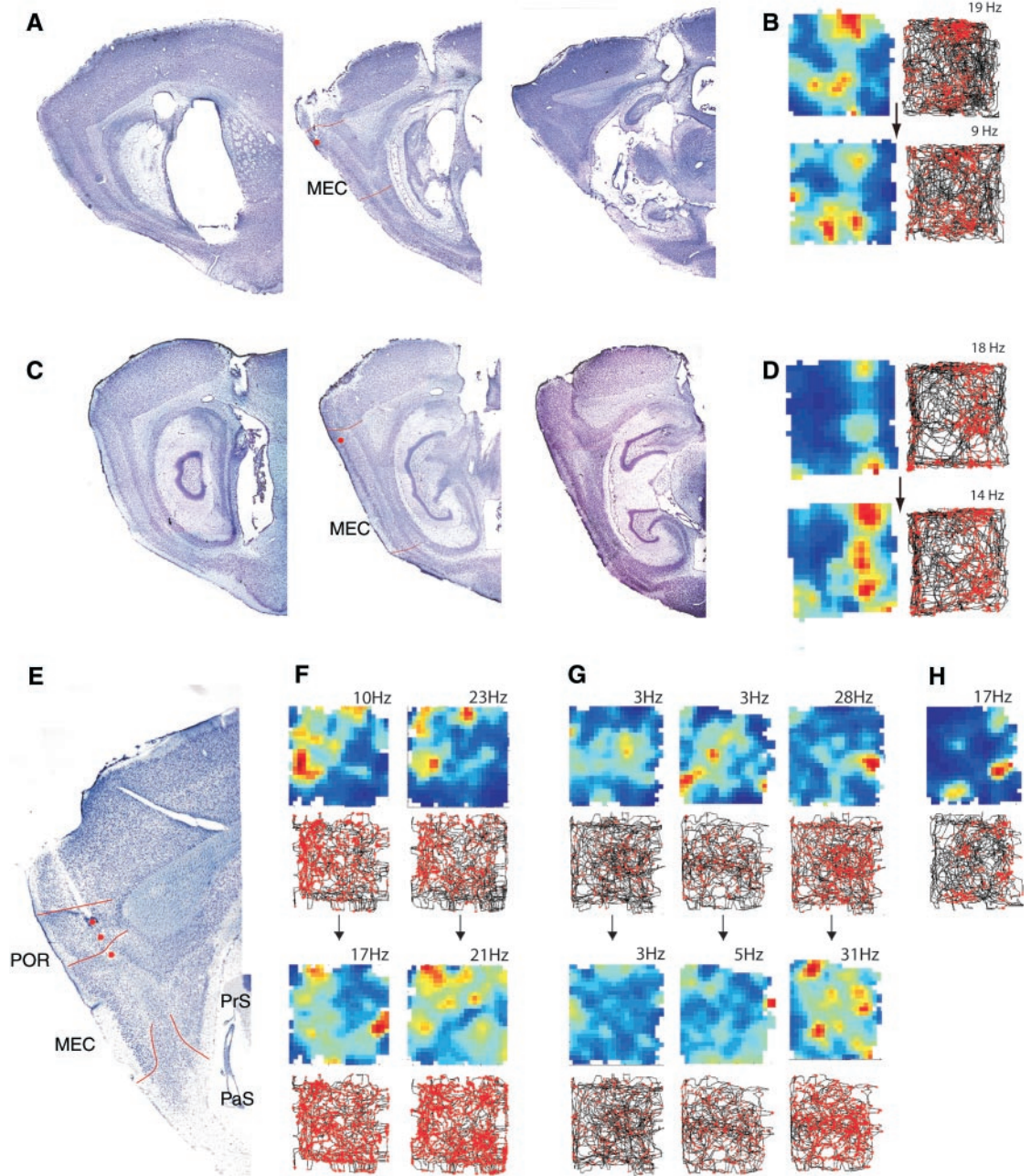
trials (pattern completion) (*32–35*). Second, firing fields in MEC were less influenced by the rat's direction of movement in a two-dimensional environment. Directional modulation in the hippocampus may arise as part of a hippocampal orthogonalization process in which incoming patterns are disambiguated from related but nonidentical patterns already stored in the network (*32, 33, 36, 37*). This process may include the separation of trajectories that run through the same location but belong to different behavioral sequences (*13, 38–40*). A hippocampal involvement in this process is consistent with the larger proportion of cells with trajectory-specific firing in deep entorhinal layers (downstream of the hippocampus) than in superficial layers (upstream of the hippocampus) (*13*). Third, the spa-

tial structure of firing was different in dorsocaudal MEC and hippocampus. How discrete and regularly spaced firing fields arise in MEC and how they transform into single-peaked representations in the hippocampus remain unresolved issues. The transformation appears to be more pronounced in the hippocampus than in the dentate gyrus, where place cells often have multiple fields (*41*).

Although the differences in stabilization and directional modulation were small, they may become more pronounced in tasks that challenge memory retrieval. The similarities in spatial coherence and information rate and the differences in stabilization and directional modulation suggest that the well-established role of the hippocampus in spatial navigation may reflect the

essential nature of spatial input as an element of most episodic memories rather than a specific role in computing the animal's location within a given context. Rather than calculating location per se, hippocampal networks may transform spatial and nonspatial sensory signals into distinguishable representations that can be retrieved despite noisy changes in background context.

References and Notes
1. W. B. Scoville, B. Milner, *J. Neurol. Neurosurg. Psychiatry* **20**, 11 (1957).
2. L. R. Squire, P. Alvarez, *Curr. Opin. Neurobiol.* **5**, 169 (1995).
3. J. L. McClelland, B. L. McNaughton, R. C. O'Reilly, *Psychol. Rev.* **102**, 419 (1995).
4. L. Nadel, A. Samsonovich, I. Ryan, M. Moscovitch, *Hippocampus* **10**, 352 (2000).

5. P. Lavenex, D. G. Amaral, *Hippocampus* **10**, 420 (2000).
6. H. Eichenbaum, *Nat. Rev. Neurosci.* **1**, 41 (2000).
7. M. P. Witter, H. J. Groenewegen, F. H. Lopes da Silva, A. H. Lohman, *Prog. Neurobiol.* **33**, 161 (1989).
8. R. D. Burwell, *Ann. N. Y. Acad. Sci.* **911**, 25 (2000).
9. J. O'Keefe, L. Nadel, *The Hippocampus as a Cognitive Map* (Clarendon, Oxford, 1978).
10. S. Wirth *et al.*, *Science* **300**, 1578 (2003).
11. C. A. Barnes, B. L. McNaughton, S. J. Mizumori, B. W. Leonard, L. H. Lin, *Prog. Brain Res.* **83**, 287 (1990).
12. G. J. Quirk, R. U. Muller, J. L. Kubie, J. B. Ranck Jr., *J. Neurosci.* **12**, 1945 (1992).
13. L. M. Frank, E. N. Brown, M. A. Wilson, *Neuron* **27**, 169 (2000).
14. R. D. Burwell, M. L. Shapiro, T. M. O'Malley, H. Eichenbaum, *Neuroreport* **9**, 3013 (1998).
15. R. D. Burwell, D. M. Hafeman, *Neuroscience* **119**, 577 (2003).
16. C. L. Dolorfo, D. G. Amaral, *J. Comp. Neurol.* **398**, 25 (1998).
17. C. L. Dolorfo, D. G. Amaral, *J. Comp. Neurol.* **398**, 49 (1998).
18. M. W. Jung, S. I. Wiener, B. L. McNaughton, *J. Neurosci.* **14**, 7347 (1994).
19. E. I. Moser, M.-B. Moser, P. Andersen, *J. Neurosci.* **13**, 3916 (1993).
20. M.-B. Moser, E. I. Moser, *Hippocampus* **8**, 608 (1998).
21. Materials and methods and additional results are available as supporting material on *Science* Online.
22. M. P. Witter, F. G. Wouterlood, P. A. Naber, T. Van Haeften, *Ann. N. Y. Acad. Sci.* **911**, 1 (2000).
23. The trajectory of a rat could be decoded from the ensemble activity of eight simultaneously recorded cells in the dorsolateral band (*21*) (movie S1). We compared the result from Bayesian decoding with a simple null model (random walk). Including unit activity in the decoding on average improved the prediction by a factor of 5.15 (*21*).
24. T. van Haeften, L. Baks-te-Bulte, P. H. Goede, F. G. Wouterlood, M. P. Witter *Hippocampus* **13**, 943 (2003).
25. V. H. Brun *et al.*, *Science* **296**, 2243 (2002).
26. This does not preclude that storage and retrieval of location are further facilitated by the transformation to single-field spatial representations in the hippocampus.
27. The reduction in spatial coherence, dispersedness, and multidirectionality may point to a role for reverberation through the entorhinal-hippocampal circuit (*42*) in refinement of firing fields in MEC, but the effects might also merely reflect global deafferentation and de-efferentation of the recorded MEC neurons.
28. T. van Haeften, F. G. Wouterlood, B. Jorritsma-Byham, M. P. Witter, *J. Neurosci.* **17**, 862 (1997).
29. J. S. Taube, R. U. Muller, J. B. Ranck Jr., *J. Neurosci.* **10**, 420 (1990).
30. L. L. Chen, L. H. Lin, E. J. Green, C. A. Barnes, B. L. McNaughton, *Exp. Brain Res.* **101**, 8 (1994).
31. J. L. Calton *et al.*, *J. Neurosci.* **23**, 9719 (2003).
32. D. Marr, *Philos. Trans. R. Soc. London B Biol. Sci.* **262**, 23 (1971).
33. B. L. McNaughton, L. Nadel, in *Neuroscience and Connectionist Theory*, M. A. Gluck, D. E. Rumelhart, Eds. (Erlbaum, Hillsdale, NJ, 1989), pp. 1–63.
34. K. Nakazawa *et al.*, *Science* **297**, 211 (2002).
35. I. Lee, D. Yoganarasimha, G. Rao, J. J. Knierim, *Soc. Neurosci. Abstr.* **91**, 11 (2003).
36. E. Bostock, R. U. Muller, J. L. Kubie, *Hippocampus* **1**, 193 (1991).
37. S. Leutgeb, K. G. Kjelstrup, A. Treves, M.-B. Moser, E. I. Moser, *Soc. Neurosci. Abstr.* **91**, 5 (2003).
38. B. L. McNaughton, C. A. Barnes, J. O'Keefe, *Exp. Brain Res.* **52**, 41 (1983).
39. A specific involvement of the hippocampus in orthogonalization of cortical input patterns is consistent with the near absence of silent cells in the MEC sample (*21*).
40. E. R. Wood, P. A. Dudchenko, R. J. Robitsek, H. Eichenbaum, *Neuron* **27**, 623 (2000).
41. M. W. Jung, B. L. McNaughton, *Hippocampus* **3**, 165 (1993).
42. T. Iijima *et al.*, *Science* **272**, 1176 (1996).
43. We thank A. Treves for discussion and L. Baks-te-Bulte, T. H. Fyhn, I. M. F. Hammer, K. Haugen, K. Jenssen, R. Skjerpeng, M. R. van der Veen, and H. Waade for technical assistance. Supported by the Norwegian Research Council (Centre of Excellence Grant) and European Commission (Framework V).

REPORTS

Search for Low-Mass Exoplanets by Gravitational Microlensing at High Magnification

F. Abe,[1] D. P. Bennett,[2] I. A. Bond,[3] S. Eguchi,[1] Y. Furuta,[1] J. B. Hearnshaw,[4] K. Kamiya,[1] P. M. Kilmartin,[4] Y. Kurata,[1] K. Masuda,[1] Y. Matsubara,[1] Y. Muraki,[1] S. Noda,[5] K. Okajima,[1] A. Rakich,[6] N. J. Rattenbury,[7]* T. Sako,[1] T. Sekiguchi,[1] D. J. Sullivan,[8] T. Sumi,[9] P. J. Tristram,[10] T. Yanagisawa,[11] P. C. M. Yock,[10] A. Gal-Yam,[12,13] Y. Lipkin,[14] D. Maoz,[14] E. O. Ofek,[14] A. Udalski,[15] O. Szewczyk,[15] K. Żebruń,[15] I. Soszyński,[15] M. K. Szymański,[15] M. Kubiak,[15] G. Pietrzyński,[15,16] L. Wyrzykowski[15]

Observations of the gravitational microlensing event MOA 2003-BLG-32/OGLE 2003-BLG-219 are presented, for which the peak magnification was over 500, the highest yet reported. Continuous observations around the peak enabled a sensitive search for planets orbiting the lens star. No planets were detected. Planets 1.3 times heavier than Earth were excluded from more than 50% of the projected annular region from approximately 2.3 to 3.6 astronomical units surrounding the lens star, Uranus-mass planets were excluded from 0.9 to 8.7 astronomical units, and planets 1.3 times heavier than Saturn were excluded from 0.2 to 60 astronomical units. These are the largest regions of sensitivity yet achieved in searches for extrasolar planets orbiting any star.

Gravitational microlensing events of high magnification occur when the foreground lens system comes into near-perfect alignment with the background source star. Suitable alignments are most readily found in the dense stellar fields in the Galactic bulge, where magnifications as high as 1000 are possible (*1*). In these events, the two images of the source star produced by the lens star merge to form a near-annular single-ring image. The events provide enhanced sensitivity for detecting planetary companions of the lens star because they can, depending on the planetary mass and position, perturb the ring-like image of the source star at times near the peak amplification (*1–5*). They complement events of low magnification that also provide substantial sensitivity for detecting extrasolar planets when "caustic crossings" occur (*6–9*). For both detection methods, the sensitivity to low-mass planets is enhanced in events with small (that is, main-sequence) source stars (*2, 5, 8*).

[1]Solar Terrestrial Environment Laboratory, Nagoya University, Nagoya 464-01, Japan. [2]Department of Physics, Notre Dame University, Notre Dame IN 46556, USA. [3]Institute of Information and Mathematical Sciences, Massey University at Albany, Auckland, New Zealand. [4]Department of Physics and Astronomy, University of Canterbury, Christchurch, New Zealand. [5]National Astronomical Observatory, Tokyo, Japan. [6]Electro Optics Systems, Canberra, Australia. [7]Department of Physics and Astronomy, University of Manchester, Manchester, UK. [8]School of Chemical and Physical Sciences, Victoria University, Wellington, New Zealand. [9]Department of Astrophysical Sciences, Princeton University, Princeton NJ 08544, USA. [10]Department of Physics, University of Auckland, Auckland, New Zealand. [11]National Aerospace Laboratory, Tokyo, Japan. [12]Department of Astronomy, California Institute of Technology, Pasadena, CA 91025, USA. [13]Hubble Fellow. [14]School of Physics and Astronomy, Raymond and Beverley Sackler Faculty of Exact Sciences, Tel-Aviv University, Tel Aviv 69978, Israel. [15]Warsaw University Observatory, Al. Ujazdowskie 4, 00-478 Warszawa, Poland. [16]Universidad de Concepcion, Departamento de Fisica, Casilla 160-C, Concepcion, Chile.

*To whom correspondence should be addressed. E-mail: njr@jb.man.ac.uk